A Prospective Comparison of Rubidium-82 PET and Thallium-201 SPECT Myocardial Perfusion Imaging Utilizing a Single Dipyridamole Stress in the Diagnosis of Coronary Artery Disease

Raymundo T. Go, Thomas H. Marwick, William J. MacIntyre, Gopal B. Saha, Donald R. Neumann, Donald A. Underwood, and Conrad C. Simpfendorfer

Departments of Nuclear Medicine and Cardiology, Cleveland Clinic Foundation, Cleveland, Ohio

The purpose of the present study is to prospectively compare myocardial perfusion imaging with rubidium-82 (^{82}Rb) by positron emission tomography (PET) with thallium-201 (^{201}Tl) imaging by single-photon emission tomography (SPECT) by recording both studies with a single dipyridamole handgrip stress, and reading both sets of images with the same display technique. In a series of 202 patients with previous coronary arteriography, the sensitivity, specificity, and accuracy of ^{82}Rb PET were 93%, 78%, and 90% and for ^{201}Tl SPECT 76%, 80%, and 77%, respectively. When 70 patients with previous therapeutic interventions were excluded, the remaining 132 patients showed a sensitivity, specificity, and accuracy of 95%, 82% and 92% for ^{82}Rb PET and 79%, 76%, and 78% for ^{201}Tl SPECT. The improved contrast resolution of PET resulted in markedly superior images and a more confident identification of defects.

J Nucl Med 1990; 31:1899–1905

The sensitivity and specificity values for the diagnosis of coronary artery disease (CAD) with positron emission tomography (PET) have been reported as high as 100% using either nitrogen-13- (^{13}N) ammonia (*1–3*) or rubidium-82 (^{82}Rb) (*4–6*). These results are superior to the values of sensitivity and specificity for thallium-201 (^{201}Tl) studies which when correlated with coronary arteriography in some recent reports showed a sensitivity and specificity range of 82%–90% and 50%–62%, respectively (*7–10*).

Received Jan. 8, 1990; revision accepted May 10, 1990.

For reprints contact: Raymundo T. Go, MD, Department of Nuclear Medicine, Gb3, Cleveland Clinic Foundation, 9500 Euclid Ave., Cleveland, OH 44195-5074.

Since many of the reported sensitivity and specificity values for ^{201}Tl were based on planar imaging, making comparison with the tomographic technique difficult, an optimal comparison of the images obtained with the two radionuclides would be to compare the sensitivity and specificity of PET with that of single-photon emission tomography (SPECT).

Recent comparison of ^{201}Tl SPECT myocardial perfusion imaging with both ^{13}N-ammonia (*11*) in 51 patients and ^{82}Rb in 60 patients (*9*) have shown sensitivities and specificities of diagnosing CAD in individual coronary arteries to be superior by PET compared with SPECT. These comparisons, however, were obtained with separate stress procedures performed within a two- (*11*) to four- (*9*) week period between the ^{201}Tl and ^{82}Rb studies but with no interval change in patient clinical status.

The present study was designed to compare the relative effectiveness of diagnosing CAD with both ^{82}Rb PET and ^{201}Tl SPECT myocardial imaging utilizing only a single dipyridamole handgrip stress and with images interpreted on identical data display techniques. In this way, any variation in the results of the two procedures would be attributable only to the inherent characteristics of the radionuclides themselves or their mechanisms of data acquisition and reconstruction.

PATIENTS, MATERIALS, AND METHODS

Patient Selection

This series consisted of 202 case studies from 209 consecutive patients referred to the PET imaging laboratory from September 13, 1988 to October 4, 1989 and having previous coronary arteriography within 6 mo of the imaging procedure. Seventy-three percent of the arteriograms were performed within 1 wk of the procedures. The seven patients excluded from the series include two cases with reconstruction artifacts

on the PET, two patients who could not be scheduled on the SPECT Triad system because of excessive weight, one patient whose coronary arteriogram was not performed in the time period, one patient who could not complete the stress protocol because of elevated blood pressure, and one patient who was administered aminophylline before the stress images were recorded.

Approximately three-quarters of the patients were classified as having significant CAD, defined as ≥50% stenosis of the luminal diameter of at least one major coronary artery as determined by subjective interpretation of coronary arteriograms by staff cardiologists performing the procedure with uniform reading standards. For patients with a patent graft around a stenosed vessel or with successful PTCA procedures, the involved vessel was considered normal. As shown in Table 1, a third of the population had undergone therapeutic intervention by either coronary bypass surgery, percutaneous transluminal coronary angioplasty, or both. In no case was the intervention after the most recent coronary arteriogram less than 3 mo prior to when the imaging studies were done.

Radiopharmaceuticals

A $^{82}Sr/^{82}Rb$ generator (Squibb Diagnostics, Inc) provided ^{82}Rb eluted with a 0.9% NaCl aqueous solution. The activity was infused into the patient by a microprocessor controlled infusion system (CTI-Siemens, Knoxville, TN) monitored by an on-line radiation detector that provided time and activity data to calculate the infused volume, total dose, and dose rate of ^{82}Rb to the patient. Typically, a fresh 110-mCi generator provided ~60 mCi ^{82}Rb in a 40–45-ml volume, and toward the end of the useful life of the generator 37–45 mCi were delivered in a 50-ml volume (*12*).

A germanium-68/gallium-68 (^{68}Ga) generator (Du Pont New England Nuclear, N. Billerica, MA) provided ^{68}Ga for transmission images of the patients in order to correct for attenuation of the ^{82}Rb images. Thallium-201 in 2–3 mCi doses was supplied as thallous chloride daily by either Mallinkrodt, Inc. (St. Louis, MO) or Du Pont NEN.

Data Acquisition

PET imaging was performed with the Posicam System (Positron Corp., Houston, TX) using a 256 × 256 matrix and obtaining 21 slices each ~5.1 mm thick. With a dose of 37–60 mCi ^{82}Rb (mean dose of 54.7 mCi) infused, a total count of 20–40 million was obtained in 4–7 min. Although the accuracy of the lower doses was not significantly different, the image quality was noticeably poorer. System sensitivity was 198K cps/μCi ^{68}Ga/cc. The attenuation correction was applied based on the transmission image in which approximately 200 million counts were recorded. Reconstruction was made by the Positron data acquisition system (PDAS, Positron Corp., Houston, TX), utilizing backprojection with a Butterworth filter of order five and cutoff of 0.4.

SPECT imaging was done with the three-headed Triad Unit (Trionix Inc., Twinsburg, OH) and recorded on a 64 × 64 matrix for 32 slices of 7.1 mm each. A dose of 2–3 mCi ^{201}Tl was administered and a total of 1.5–4 million counts recorded in 9–14 min with a low-energy all-purpose collimator. The counts per slice ranged from 100–200 thousand, which is considered sufficient for cardiac reconstruction with a smoothing filter such as Hamming (*13,14*). Attenuation correction was calculated by determining the scan orbit boundary (*15*) to determine the distance to modify the backprojection, assuming an attenuation coefficient of 0.14. Reconstruction was performed by the Sun computer on the Triad by backprojection using a Hamming filter with a cutoff of 0.7. A comparison of these techniques is shown in Table 2.

TABLE 1
Patient Population

Myocardial infarction	
None	107
Yes	95
Total	202
Therapeutic intervention	
None	132
Bypass	37
PTCA	30
Both	3
Total	202
Coronary angiography classification*	
Normal and nonsignificant (CAD) (<50%) or patent graft or affected vessel	50
Significant CAD (≥50%)	152
Total	202
Number of vessels involved	
Single	50
Double	55
Triple	47
Total	152

* Subjective interpretation of coronary angiography.

TABLE 2
Data Acquisition

	^{201}Tl SPECT	^{82}Rb† PET
Imaging system	Triad*	Posicam‡
Computers	SUN-VAX 780	PDAS‡ MicroVAX II
Data sampling	360°	3-D
Matrix size	64 x 64	256 x 256
Acquisition time stress	9 min	4 min
Redistribution or rest	14 min	7 min
Total counts	1.5–4M	20–40M
Counts/slice over heart	100–200K	1–2M
Number of slices	32 (FOV)	21 (FOV)
Slice thickness	7.1 mm	5.1 mm
Reconstruction	Backprojection	Backprojection
Filter	Hamming, cutoff 0.7	Butterworth, order 5, cutoff 0.4
Attenuation correction	Image orbit boundary (calculated)	Transmission image (measured)

* Trionix, Inc.
† Squibb Diagnostics.
‡ Positron Corp.

Imaging Protocol

Each patient had monitoring of ECG, blood pressure, temperature, and pulse during the PET study. Accurate localization of the heart prior to imaging was accomplished by marking the lower border of the heart fluoroscopically. A transmission image was then obtained with the plexiglass ring filled with 3–4 mCi ^{68}Ga. Following the transmission image, 40–60 mCi ^{82}Rb were injected into the patient through the infusion line over a period of ~30–60 sec, depending on the strength of the generator. After a delay of 45–65 sec, data were collected for the resting image over a period of 7 min. After the resting ^{82}Rb image was obtained, dipryidamole was infused by the method of Gould (*5,16*) at a dose rate of 0.142 mg/kg/min for 4 min to induce coronary vasodilatation, while continuously monitoring and recording the ECG and other vital signs. The patient started isometric hand-grip exercise at 25% maximum strength at 2 min after the completion of dipyridamole infusion. At 4 min after the end of the dipyridamole infusion, 40–60 mCi ^{82}Rb was infused while maintaining the hand-grip for an additional 2 min. Stress ^{82}Rb image data were collected starting 45–65 sec after the administration of the tracer for a period of 4 min in the same manner as in the case of resting images.

Immediately following the stress ^{82}Rb data acquisition, 2–3 mCi ^{201}Tl were injected through the infusion line and, within 10 min after the ^{201}Tl injection, stress ^{201}Tl SPECT data acquisition was initiated using the Triad camera. Redistribution ^{201}Tl SPECT images were recorded 3–4 hr later. Intravenous aminophylline was available as an antidote to counteract significant adverse reactions as a result of dipyridamole infusion.

The sequential time elapsing for the entire protocol is shown in Table 3.

Image Display and Interpretation

The original slices of reconstructed image data were transferred from the PDAS (PET) and SUN (SPECT) computers to a VAX 11/750 computer for reorientation of the data from body axis to a cardiac-axis orientation for display of the short-axis, vertical long-axis, and horizontal long-axis. Displays of the PET stress and rest images, or SPECT stress and equilibrium image slices were viewed simultaneously on a split monitor and a reference slice of an orthogonal cardiac axis was included to verify that the stress and rest images were identical slices. Each series was under separate control so that either stress or redistribution or rest slices could be adjusted for accurate alignment and comparison.

Images were displayed with a choice of a continuous rainbow color band for localizing the myocardial edges and segmented color scales of 10% (*17*) and 5% differences for quantitative interpretation. The three color scales are illustrated in Figure 1. The quantitative color scales are used to grade the images as discussed below.

Myocardial segments were considered normal if the count variation between segments was within 20% (*18*) or less when compared to the segment with the highest count rate for each radionuclide. For the apex and diaphragmatic segments, a higher range of decreased counting rate variation of 30%–40% was allowed for ^{201}Tl and 20%–30% for ^{82}Rb. Normal myocardial segments show a gradual decrease in radioactivity while abnormal myocardial segments with perfusion abnormality show an abrupt and sustained decrease in radioactivity along an involved segment.

Myocardial ischemia was designated for segments with a decrease in counting rate more than the above normal limits on stress images, with the segments increasing in relative activity at rest or redistribution by 20% (*18*) or more. If the segment filled in with activity at levels less than 20%, scar was designated. For a true abnormality to be so designated, it must be seen on two consecutive slices and preferably verified in an orthogonal plane.

Interpretations were made using the quantitative color scale data of the three cardiac tomographic planes. The reader was blinded to the patient's clinical history or findings on the coronary arteriograms.

TABLE 3
Sequence and Timing of Combined ^{201}Tl and ^{82}Rb Myocardial Perfusion Protocol

Time in minutes	
0–25	Heart border identified by fluoroscopy, patient positioned on PET table
25–45	Acquire ^{68}Ga transmission scan for attenuation correction
45–55	Remove ^{68}Ga ring, start infusion of ^{82}Rb
55–62	Acquire ^{82}Rb rest image
62–66	Infuse dipyridamole (0.142 mg/kg/min)
68–72	Apply handgrip
70–72	Infuse ^{82}Rb (40–60 mCi)
72–76	Acquire ^{82}Rb stress image
76	Inject bolus ^{201}Tl (2–3 mCi)
80–89	Acquire ^{201}Tl stress image
270–284*	Acquire ^{201}Tl redistribution image

* 3–4-hr time delay for ^{201}Tl redistribution image.

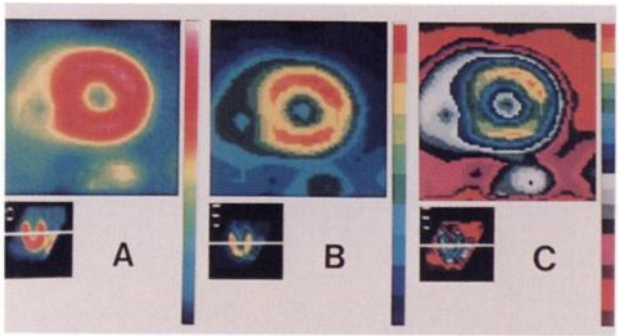

FIGURE 1
Three color scales applied to the same short-axis cardiac tomographic slice: the continuous rainbow color band on left (A), the 10% segmented quantitative scale in middle (B), and the 5% segmented quantitative scale on the right (C). Note vertical long-axis reference slice localization image at lower left of each short-axis image showing to which level of the left ventrical the short-axis slice corresponds. For all succeeding figures, the 10% color scale is used. Orientation of short-axis is anterior (top), septum (left), lateral wall (right), and inferior (bottom).

TABLE 4
Comparative Sensitivity and Specificity of Total Population Studied (n = 202)

	^{201}Tl SPECT	^{82}Rb PET	p value
Sensitivity	115/152 (76%)	142/152 (93%)	<0.001
Specificity	40/50 (80%)	39/50 (78%)	n.s.
Accuracy	155/202 (77%)	181/202 (90%)	<0.001

n.s. = nonsignificant.

RESULTS

Sensitivity and Specificity

The comparison of the total population studied on 202 patients showed a sensitivity, specificity, and accuracy of 93%, 78% and 90%, respectively, for ^{82}Rb and 76%, 80%, and 77% for ^{201}Tl (Table 4).

True-Positive Readings

An example of myocardial ischemia involving the lateral and posterolateral segments displayed in all three tomographic planes on the ^{82}Rb and ^{201}Tl images is illustrated in Figure 2. The areas with ischemia are best appreciated in the short-axis and horizontal long-axis slices, noting the transitory nature of the abnormality between the stress and rest or redistribution studies.

An abnormal case demonstrating myocardial scar of the inferior and posterior segments on both the ^{82}Rb and ^{201}Tl images is illustrated in Figure 3. The persistent abnormalities of the inferior and posterior segments are best demonstrated in the short-axis and vertical long-axis slices. In the horizontal long-axis, the displayed slice is diaphragmatic so that little activity is visualized except at the inferoapical and inferolateral regions.

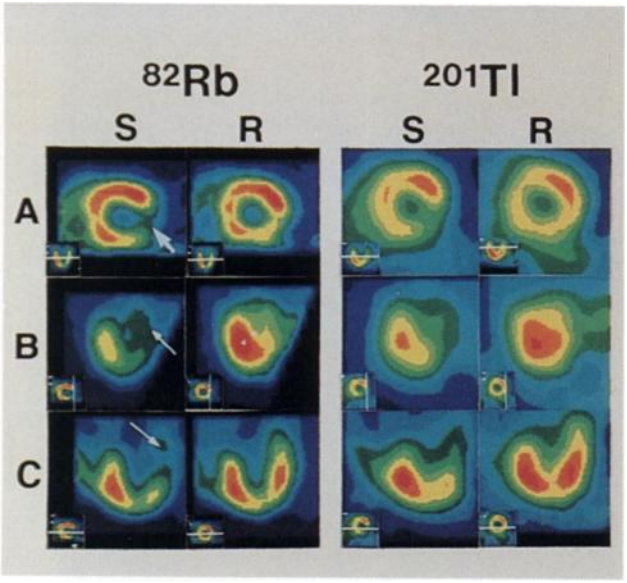

FIGURE 2
Comparison of ^{82}Rb and ^{201}Tl images of a patient with ischemia involving the lateral (thick arrow) and posterolateral (thin arrows) segments. Note reference slice localization images which demonstrate the stress (S) and rest (R) ^{82}Rb images and the stress (S) and redistribution (R) ^{201}Tl images were taken at the same slice. Note decreased activity on lateral wall of 50% on the ^{82}Rb stress images and 40% on the ^{201}Tl stress images, but filling-in to a normal 20% at rest or redistribution indicative of ischemia. Row A = cardiac short-axis with orientation described in caption of Figure 1. Row B = vertical long-axis, anterior wall on left, and posterior wall on right. Row C = horizontal long-axis, septum on left, and lateral wall on right.

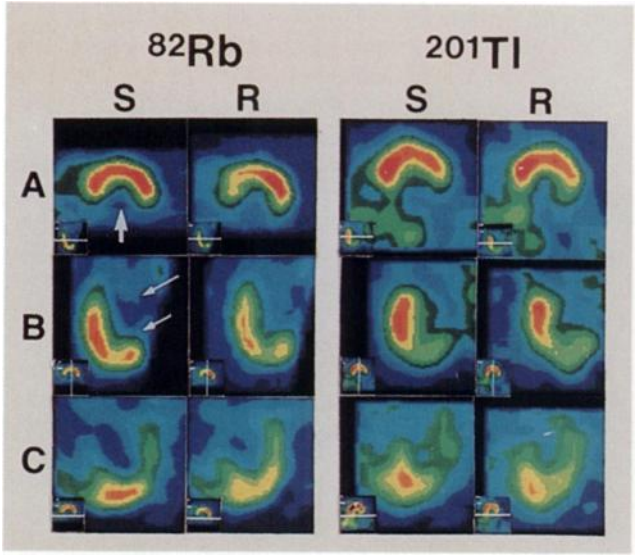

FIGURE 3
Comparison of ^{82}Rb and ^{201}Tl images of a patient with diaphragmatic wall scar (thick arrow). Further division into inferior (short thin arrow) and posterior (long thin arrow) wall involvement is seen best in the vertical long-axis slice. Although the appearance of the ^{82}Rb images is superior, the diagnosis is identical with both the PET and SPECT images. Note an 80% decrease in counts at the diaphragmatic wall on the ^{82}Rb image and a 60% decrease on the ^{201}Tl image consistent with scar. Row A = cardiac short-axis. Row B = vertical long-axis, Row C = horizontal long-axis. S = stress and R = rest or redistribution. Orientation is described in Figure 2.

False-Negative Readings

In the group of patients with abnormal coronary arteriograms, ten patients were false-negative by both ^{201}Tl and ^{82}Rb studies. Of these ten, four had single-vessel stenoses of 50% on the coronary arteriograms and two had critical CAD but with well established collaterals to the area supplied by the stenosed vessel. Of the remaining four cases, three had right coronary artery stenoses of 60%–80% and the remaining case involved both patent and occluded grafts.

There were no false-negative cases diagnosed by the ^{82}Rb technique that were correctly diagnosed by ^{201}Tl. However, 27 cases were incorrectly diagnosed as negative by ^{201}Tl that were correctly diagnosed positive by ^{82}Rb. As discussed by Marwick et al. (*19*), 21 of the 27 cases involved the inferior and posterior wall. Of these, 8 of 21 cases showed a transient defect indicating ischemia as illustrated in Figure 4 and 13 of 21 cases showed a fixed defect indicating scar as illustrated in Figure 5. Note that all these abnormalities were detected by the ^{82}Rb PET images only.

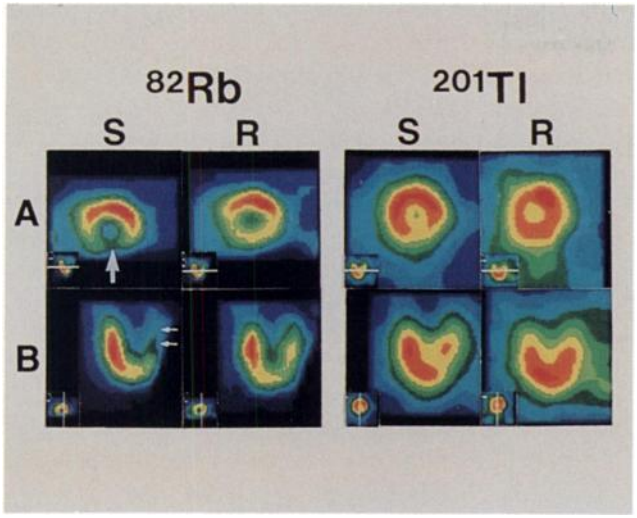

FIGURE 4
Comparison of ^{82}Rb and ^{201}Tl images of a patient with inferior wall ischemia as displayed on the short-axis slice (thick arrow) and vertical long-axis slice (thin short arrows). The inferior wall on the ^{82}Rb stress image shows a decrease to 50% count at stress and only to 20% at rest indicating ischemia. However, the ^{201}Tl stress image does not decrease more than 20% and, thus, is read as normal. Row A = cardiac short-axis, Row B = vertical long-axis. Stress = stress and R = rest or redistribution. Orientation is described in Figure 2.

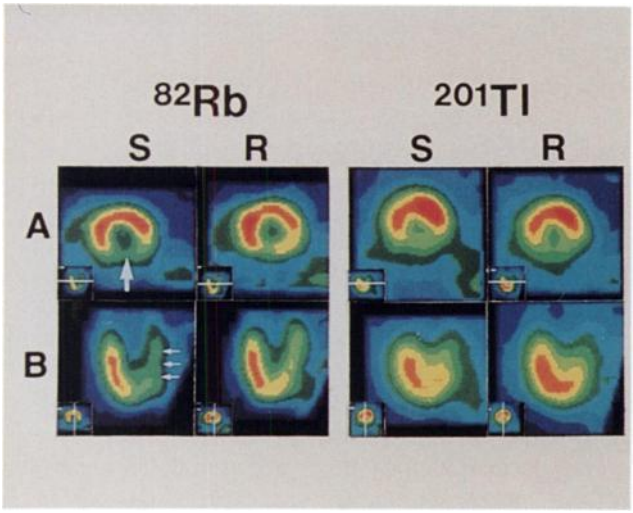

FIGURE 5
Comparison of ^{82}Rb images on a patient with inferior wall scar (thick arrow) correctly diagnosed by ^{82}Rb images but showing false negative results with ^{201}Tl. The inferior wall of the ^{201}Tl images shows a decrease in radioactivity but this decrease does not have sufficient contrast differential to be beyond normal variation. On the vertical long-axis slice, the diaphragmatic segments on the ^{82}Rb stress image show an abrupt and sustained decreased activity to 40% which is an abnormal pattern but the same area on the ^{201}Tl image shows pattern of a gradual decrease in count which is normal. Row A = cardiac short-axis, Row B = vertical long-axis slices. S = stress and R = rest or redistribution. Orientation is described in Figure 2.

False-Positive Readings

Of the total thirteen cases of false-positive studies, six were false-positive both on the ^{82}Rb and ^{201}Tl images; five were false-positive on the ^{82}Rb image alone.

Of the eleven cases that were false-positive on ^{82}Rb, three with fixed defects had previous PTCA for significant CAD, one had a documented previous myocardial infarction, two had non-Q-wave myocardial infarction, two had aortic valve disease, and one had primary myocardial disease. The remaining two subjects had no history that could be correlated with the positive reading.

Three cases that were false-positive on the ^{201}Tl image but normal on the ^{82}Rb were considered to be so due to breast attenuation as illustrated in Figure 6 and diaphragmatic wall attenuation artifacts.

As discussed in the selection of patients, about one-third of the population had previous bypass surgery or angioplasty or both. Since the classification of CAD was based entirely on the status of the coronary vessels in the most recent arteriogram, the actual presence of previous infarctions was not taken into consideration during correlation and data analysis of the results. If this group of 70 patients that had previous therapeutic interventions were omitted from the total population, analysis of the remaining 132 patients showed a sensitivity, specificity, and accuracy of 95%, 82%, and 92% for ^{82}Rb PET and 79%, 76%, and 78% for ^{201}Tl SPECT (Table 5).

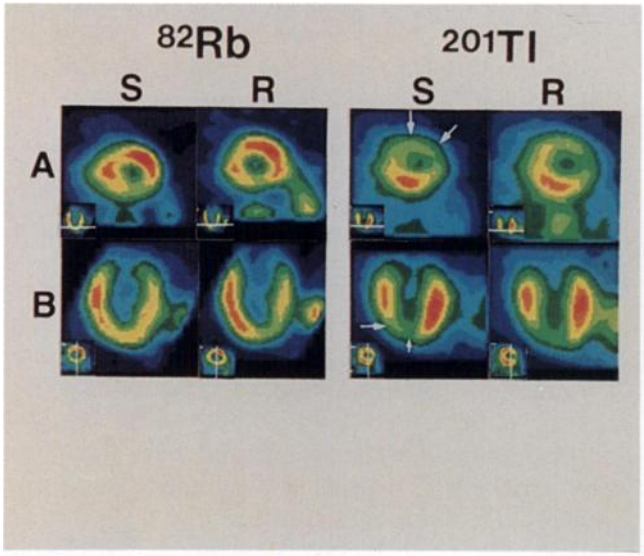

FIGURE 6
The ^{82}Rb image on the left shows normal radioactivity distribution but the ^{201}Tl image on the right shows fixed defects at the distal anterior and distal anterolateral (long bigger arrows) as well as the apical (short small arrow) segment with decreased activity up to 30%–40% most likely due to breast attenuation. The coronary angiogram was normal. Row A = cardiac short-axis; Row B = vertical long-axis slices. S = stress and R = rest or redistribution. Orientation is described in Figure 2.

TABLE 5
Comparative Sensitivity and Specificity of Patients Without Bypass or Angioplasty (n = 132)

	^{201}Tl SPECT	^{82}Rb PET	p value
Sensitivity	77/98 (79%)	93/98 (95%)	0.002
Specificity	26/34 (76%)	28/34 (82%)	n.s.
Accuracy	103/132 (78%)	121/132 (92%)	0.002

n.s. = nonsignificant.

DISCUSSION

Comparing the sensitivity of the two imaging techniques, it is evident that it is the interpretations at the regions of the inferior and posterior walls that are primarily responsible for the reduced sensitivity of the ^{201}Tl imaging when compared with the ^{82}Rb method (*19*). It was considered possible that the failure to visualize the transient defects on the ^{201}Tl SPECT images may indicate a lack of sufficient stress induced by dipyridamole. The recent review of Leppo (*20*), however, shows little difference in ^{201}Tl imaging sensitivity between exercise stress and dipyridamole technique. In addition, the 1,096 patient study comparing dipyridamole ^{201}Tl studies with coronary arteriography as quoted by Kuhl et al. (*7*) showed a similar sensitivity of 85%.

In terms of experimental design, it would have been preferable to inject the ^{82}Rb and ^{201}Tl at the same time following the dipyridamole administration. Constraints of the IND, however, required a separation between administrations of the two radiotracers. The 5-min separation in time between the injection of ^{82}Rb and ^{201}Tl was not considered to be a disadvantage because the time duration of the dipyridamole-induced coronary vasodilatation is sufficiently persistent over this time interval (*21,22*). The study of Rossen et al. (*22*) also showed that handgrip did not change the effect of dipyridamole.

The failure of the ^{201}Tl images to display an even greater number of cases with persistent defects along the inferior and posterior walls, however, indicates that this problem is independent of the stress status of the coronary vessels.

A more important factor responsible for the lower sensitivity with ^{201}Tl imaging is considered to be the problem of attenuation and scatter. It is believed that the less accurate attenuation correction in SPECT and the larger reduction in the scatter fraction achieved by using 511 keV annihilation photons rather than the 60–80 keV X-rays of ^{201}Tl combine to give a much improved contrast resolution with ^{82}Rb images. This improvement is most apparent in the inferior and posterior myocardial wall, which is deeper in the thorax and more subject to the effects of both attenuation and scatter with SPECT.

The specificity values of both ^{82}Rb and ^{201}Tl were somewhat lower than had been previously reported and were thought to be primarily due to the patient population selected. The requirement of the protocol that only patients with a recent coronary arteriogram be accepted in the study has resulted in a population with a high probability of cardiac disease present at that time. In the sub-population of 50 patients classified as normal or subcritical CAD, 13 had undergone prior PTCA including three with multiple procedures. No patient, however, had undergone PTCA closer than four months to the time of imaging.

In addition, myocardial infarction with a normal coronary arteriogram is not an uncommon clinical entity (*23*) and can cause abnormal myocardial perfusion images. Valvular disease (*24*) and primary myocardial disease (*25*) without concomitant CAD have also been reported to cause abnormal ^{201}Tl myocardial perfusion images. As reported in the results, only 2 patients of the 13 false-positive did not fall into any one of these possible categories.

A final factor that may affect both sensitivity and specificity is that the coronary arteriograms were interpreted and reported by subjective reading, so that high reliance would be lacking in these critical cases with borderline stenosis. Overestimation of stenotic lesions and the lack of accuracy in predicting significant decrease in coronary flow in borderline stenoses has been previously reported (*26*). Digital arteriography may have helped somewhat but may still be subject to the same variability (*27*).

Although the population of this comparison included patients with other types of cardiac diseases besides CAD, this factor was considered desirable since it is typical of the type of referrals encountered in a hospital referral base. Considering our hospital setting, the sensitivity and specificity values obtained here for ^{82}Rb PET were quite similar to those values reported by the previously cited hospital-based study at the University of Michigan (*9*). For the ^{201}Tl SPECT studies, our sensitivity was less, specificity was greater, but accuracy was the same. It must be realized that in any sensitivity and specificity study, the decision distinguishing normal from abnormal readings may vary among institutions and the comparisons of the accuracy values may be more meaningful.

CONCLUSIONS

For the population of 202 patients studied, the sensitivity of ^{82}Rb PET imaging for the diagnosis of CAD has been demonstrated to be significantly improved over the sensitivity of ^{201}Tl SPECT imaging in patients with and without previous bypass surgery or PTCA. The difference in specificity between ^{82}Rb and ^{201}Tl is slight.

The improvement in sensitivity by ^{82}Rb PET over

^{201}Tl SPECT imaging is more related to contrast resolution rather than spatial resolution. The improvement in contrast resolution in the PET technique due to reduction of scatter and improved attenuation correction with 511 keV annihilation photons has resulted in greatly improved images, thus resulting in superior detection of segmental perfusion abnormalities.

For this population, the ^{82}Rb specificity was not improved over ^{201}Tl, although the ability of PET imaging to eliminate soft-tissue attenuation had been demonstrated. This is probably due to the inclusion of patients who have normal coronary angiograms but have had previous myocardial infarctions and patients who have cardiac disease other than CAD that can cause false-positive abnormalities on the radionuclide perfusion image.

ACKNOWLEDGMENTS

The authors wish to thank Janet L. King, RN, ARRT and Annette Beachler, CMNT for their skillful and meticulous performance of the PET protocol and data acquisition, without which the comparison would not have been meaningful. We also wish to thank Sandra K. Petraus and Donna Fisher for the preparation of this manuscript.

Presented in part at the 36th Annual Meeting of the Society of Nuclear Medicine, June 13–16, 1989, St. Louis, Missouri.

REFERENCES

1. Schelbert HR, Wisenberg G, Phelps ME, et al. Noninvasive assessment of coronary stenosis by myocardial imaging during pharmacologic coronary vasodilatation. VI. Detection of coronary artery disease in man with intravenous NH_3 and positron computed tomography. *Am J Cardiol* 1982; 49:1197–1207.
2. Tamaki N, Yonekura Y, Senda M, et al. Myocardial positron computed tomography with ^{13}N-ammonia at rest and during exercise. *Eur J Nucl Med* 1985; 11:246–251.
3. Senda M, Yonekura Y, Tamaki N, et al. Interpolating scan and oblique-angle tomograms in myocardial PET using nitrogen-13-ammonia. *J Nucl Med* 1986; 27:1830–1836.
4. Selwyn AP, Allan RM, L'Abbate AL, et al. Relation between regional myocardial uptake of rubidium-82 and perfusion: absolute reduction of cation uptake in ischemia. *Am J Cardiol* 1982; 50:112–131.
5. Gould KL, Goldstein RA, Mullani NA, et al. Noninvasive assessment of coronary stenoses by myocardial perfusion imaging during pharmacologic coronary vasodilation. VIII. Clinical feasibility of positron cardiac imaging without a cyclotron using generator-produced rubidium-82. *J Am Coll Cardiol* 1986; 7:775–789.
6. Williams BR, Jansen D, Wong LF, Fiedotin AJ, Knopf WD, Toporoff SJ. Positron emission tomography for the diagnosis of coronary artery disease: a non-university experience and correlation with coronary angiography [Abstract]. *J Nucl Med* 1989; 30:845.
7. Kuhl DE, Wagner Jr HN, Alavi A, et al. Positron emission tomography: clinical status in the United States in 1987. *J Nucl Med* 1988; 29:1136–1143.
8. Van Train KF, Berman DS, Garcia EV, et al. Quantitative analysis of stress thallium-201 myocardial scintigrams: a multicenter trial. *J Nucl Med* 1986; 27:17–25.
9. Stewart RE, Kalus ME, Molina E, et al. Rubidium-82 PET versus thallium-201 SPECT for the diagnosis of regional coronary artery disease [Abstract]. *Circulation* 1989; 80:II-201.
10. Iskandrian AS, Heo J, Kong B, Lyons E. Effect of exercise level on the ability of thallium-201 tomography imaging in detecting coronary artery disease: analysis of 461 patients. *J Am Coll Cardiol* 1989; 14:1477–1486.
11. Tamaki N, Yonekura Y, Senda M, et al. Value and limitation of stress thallium-201 single-photon emission computed tomography: comparison with nitrogen-13-ammonia positron tomography. *J Nucl Med* 1988; 29:1181–1189.
12. Saha GB, Go RT, MacIntyre WJ, et al. Use of Sr-82/Rb-82 generator in clinical PET studies. *Nucl Med Biol* 1990:in press.
13. MacIntyre WJ, Go RT, Houser TS. Cardiac tomography: techniques and applications. In: Spencer RP, ed. *New procedures in nuclear medicine.* Boca Raton: CRC Press, Inc.; 1989:129–142.
14. Budinger TF, Derenzo SE, Greenberg WL, Gulberg GT, Huesman RH. Quantitative potentials of dynamic emission computed tomography. *J Nucl Med* 1978; 19:308–315.
15. Lim CB, Gottschalk S, Walker R, et al. Triangular SPECT system for 3-D total organ volume imaging: design concept and preliminary imaging results. *IEEE Trans Nucl Sci* 1985; NS-32:741–747.
16. Demer LL, Gould KL, Goldstein RA, et al. Assessment of coronary artery disease severity by positron emission tomography. *Circulation* 1989; 79:825–835.
17. Go RT, MacIntyre WJ, O'Donnell JK, et al. Transaxial single-photon emission computed tomographic myocardial imaging with ^{201}Tl: instrumentation, technical, and clinical aspects. In: Freeman LM, Weissman HS, eds. *Nuclear medicine annual 1985.* New York: Raven Press; 1985:171–198.
18. Go RT, MacIntyre WJ. Myocardial perfusion imaging. In: Yeh SDJ, Chen DCP, eds. *Nuclear medicine update 1988.* Taipei: The Society of Nuclear Medicine ROC; 1988:152–164.
19. Marwick TH, Go RT, Rehm PJ, Underwood DA, MacIntyre WJ. Comparison of Rb-82 PET and Tl-201 SPECT. Frequency and causes of disparate results [Abstract]. *Circulation* 1989; 80:II–209.
20. Leppo JA. Dipyridamole-thallium imaging: the lazy man's stress test. *J Nucl Med* 1989; 30:281–287.
21. Brown BG, Josephson MA, Peterson RB, et al. Intravenous dipyridamole combined with isometric handgrip for near maximal acute increase in coronary flow in patients with coronary artery disease. *Am J Cardiol* 1981; 48:1077–1085.
22. Rossen JD, Simonetti I, Marcus ML, Winniford MD. Coronary dilation with standard dose dipyridamole and dipyridamole combined with handgrip. *Circulation* 1989; 79:566–572.
23. Raymond RE, Lynch J, Underwood DA, Leatherman J, Razavi M. Myocardial infarction and normal coronary arteriography: a 10-year clinical and risk analysis of 74 patients. *J Am Coll Cardiol* 1988; 11:471–477.
24. Bailey IK, Come PC, Kelly DT, Barow RD, Griffith LSC, Strauss HW. Thallium-201 myocardial perfusion imaging in aortic valve stenosis. *Am J Cardiol* 1977; 40:889–899.
25. Bulkley BH, Hutchins GM, Bailey I, Strauss HW, Pitt B. Thallium-201 imaging and gated cardiac blood-pool scans in patients with ischemic and congestive cardiomyopathy: a clinical and pathologic study. *Circulation* 1977; 55:753–761.
26. White CW, Wright CB, Doty DB, et al. Does visual interpretations of the coronary arteriograms predict the physiologic importance of the coronary stenosis. *N Engl J Med* 1984; 310:819–824.
27. Gurley JC, Nissen SE, Booth DC, et al. Comparison of simultaneously performed digital and film-based angiography in assessment of coronary artery disease. *Circulation* 1988; 93:1411–1420.